Focal Adhesion Induction at the Tip of a Functionalized Nanoelectrode

Daniela E. Fuentes,[1] Chilman Bae,[2] and Peter J. Butler[1]

[1]Department of Bioengineering, The Pennsylvania State University, 205 Hallowell Building, University Park, PA 16802, USA; and [2]Center for Single Molecule Biophysics, University at Buffalo, State University of New York, 301 Cary Hall, Buffalo, NY 14214, USA

Associate Editor Edward Guo oversaw the review of this article.

Abstract—Cells dynamically interact with their physical micro-environment through the assembly of nascent focal contacts and focal adhesions. The dynamics and mechanics of these contact points are controlled by transmembrane integrins and an array of intracellular adaptor proteins. In order to study the mechanics and dynamics of focal adhesion assembly, we have developed a technique for the timed induction of a nascent focal adhesion. Bovine aortic endothelial cells were approached at the apical surface by a nanoelectrode whose position was controlled with a resolution of 10 s of nanometers using changes in electrode current to monitor distance from the cell surface. Since this probe was functionalized with fibronectin, a focal contact formed at the contact location. Nascent focal adhesion assembly was confirmed using time-lapse confocal fluorescent images of red fluorescent protein—tagged talin, an adapter protein that binds to activated integrins. Binding to the cell was verified by noting a lack of change of electrode current upon retraction of the electrode. This study demonstrates that functionalized nanoelectrodes can enable precisely-timed induction and 3-D mechanical manipulation of focal adhesions and the assay of the detailed molecular kinetics of their assembly.

INTRODUCTION

There exist many force spectroscopy techniques that can be used to characterize and manipulate single cells. These include atomic force microscopy (AFM),[6,21,48] optical tweezers,[11,31,50,58] magnetic tweezers,[12,27,45,56] biomembrane force probes,[22] and micro-needle manipulation.[16] Each of these methods is well suited to a particular force magnitude and positional accuracy and, collectively, they have contributed immensely to our understanding of how cells sense force and how they exert forces on their surroundings. Such data has led to a detailed delineation of the mechanisms cells use to organize their environment, an organization which leads to physiological phenomena including bone remodeling, blood vessel caliber control, and embryonic development[44] and pathophysiological phenomena such as cancer, atherosclerosis, hypertension, and arthritis.[19] Although force spectroscopy has become ubiquitous because of its potential to uncover details of mechanobiology, there remain some needed functionalities. First, it would be advantageous to define the precise timing of the transition between non-contact and contact of the force probe with the cell so that molecular assembly kinetics resulting from initial contact could be measured. Second, the probe site should be on the order of the typical size of a focal adhesion, which is a micron or less. Third, the system should be able to apply prescribed deformations to cells at a prescribed location in order to test the hypothesis that mechanically-induced changes in cells are spatially heterogeneous. The technique to accomplish these design goals must be compatible with multiple microscopy imaging techniques and be able to be implemented in an environmentally controlled cellular sample chamber, in order to maintain cells under physiological conditions. One imaging modality that can delineate cell surface topography at the nanometer level is scanning ion conductance microscopy (SICM).[28] In this method an electrode is brought close to a sample, and scanned laterally. During this scanning, the electrode current is read continuously and the pipette position is controlled in a feedback manner to maintain constant electrode distance from the sample. Motions necessary to maintain ion current are converted to sample topography. The lateral spatial resolution of this method is limited primarily by the size of the pipette tip, which can be as small as 10 nm, and the axial resolution (distance from cell) can be as small as

10 s of nm subject only to the ability to measure small current flow through the electrode. Thus, SICM provides a means to have nanometer-scale topographical information in a non-contact mode.[34] Use of a non-contact mode has a particular advantage since cellular topography can be imaged over many hours without damaging the cells and without inducing changes in the cell that might be related to contact and force application.[25]

To date there are no reports on the use of SICM with functionalized electrodes. Such an innovation could assist in assessing the role of adhesion events in a number of contexts. In addition, taking advantage of SICM's ability to detect distance from current means that contact timing and location can be quantified and prescribed. This method would enable experiments that seek to test the role of contact and deformation on the kinetics of reactions on the surface and inside cells. In this study we have developed such a tool. By functionalizing a SICM nanoprobe with fibronectin and mounting the system on a high speed confocal microscope we show that we can induce nascent focal adhesion formation on the apical surface of a cell with precise timing and position. Furthermore, by transfecting the cell with fluorescent focal adhesion proteins, we show that the dynamics of protein recruitment can be assessed from the moment of contact onward. Such information will allow us in future studies, to determine the precise kinetic parameters related to molecular transport to focal adhesions. Furthermore, we show that prescribed deformations can be applied to the cells. Such deformations should yield insight into long-range coupling of cellular constituents as well as provide the capability to assess the role of deformation in the kinetics of focal adhesion assembly.

MATERIALS AND METHODS

Experimental Setup

A schematic representation of the experimental setup is shown in the Fig. 1 (top). Bovine aortic endothelial cells (BAECs) were cultured and plated on a temperature-controlled chamber (Bioptechs, Butler, PA, USA) and placed on a piezoelectric stage with resolution of 0.2 nm and 100 μm range of motion (NanoView & NanoDrive, Mad City Labs, Madison, WI, USA), which was, in turn, mounted on a joystick-controlled xy stage with 20 nm resolution and 25 mm range of motion (Mad City Labs Inc., Madison, WI, USA). Both stages were controlled with dedicated LabVIEW-based software programs. The piezoelectric stage was also controlled by Voxcell imaging software (Visitech International, Sunderland, UK).
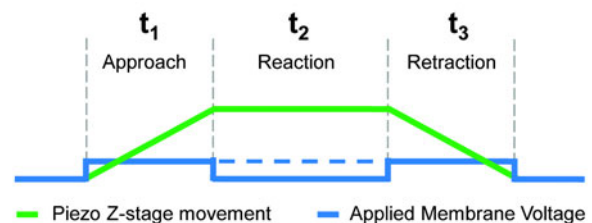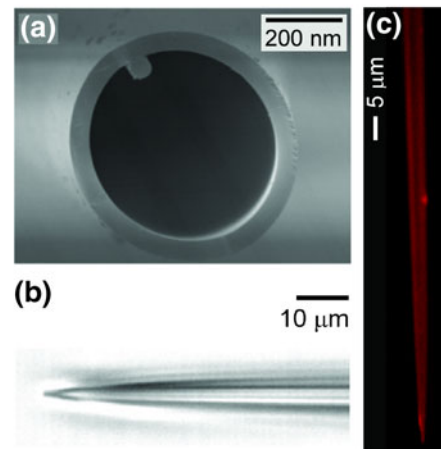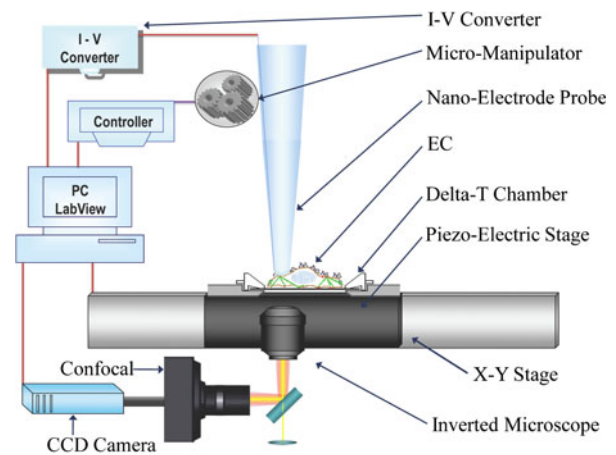
FIGURE 1. Top: Experimental setup. Middle: Probe Development. (a) Electron micrograph of tip and probe at 69,000× magnification displays an inner radius of 252 nm. (b) Phase contrast images of probe. (c) Fluorescence Microscopy image of functionalized probe. Fibronectin labeled with Alexa-Fluor 568 allows visualization of functionalized probe. Bottom: Probe voltage and cell positioning sequence. Time sequences of piezoelectric stage in z-direction movement (green line) and applied voltage by the probe (blue line), x-axis = time. t_1: *approach phase*: the stage moved the cell closer to the probe while the nanoelectrode applied a constant voltage. t_2: *reaction phase*: once in contact, the stage was not moved, allowing the functionalized probe to react with the cell. Voltage was (dashed blue line) or was not (solid blue line) applied during this phase. t_3: *retraction phase*: the stage was moved such that the probe-cell distance increased. During this phase, the nanoelectrode applied a constant voltage.

An inverted Olympus IX71 microscope with a 100 W halogen light provided brightfield illumination for phase contrast which was used for initial positioning of the

probe. Imaging was done with an oil-immersion objective (PlanAPO N 60X/1.45 NA, TIRFM-2, WD 0.15 mm). A multibeam laser confocal scanner (VT-Infinity3; Visitech International, Sunderland, UK) was used to visualize the real-time changes of fluorescence in cells. A high-performance electron multiplying cooled charge-coupled device (EMCCD) digital imaging camera (Sensicam-EM; Cooke Corporation, Romulus, MI, USA) performed image capture.

The nanoelectrode probe was mounted on a computer-controlled micromanipulator (MP-285; Sutter Instruments, Novato, CA, USA). A patch clamp amplifier (Model 2400, A-M Systems, Inc., Carlsborg, WA, USA) with a 20 MΩ probe were used to monitor current changes through the nanoelectrode and to apply computer-controlled external voltages to it. A LabVIEW-based software program that received data from a data acquisition board (NI PCI 6229, National Instruments, Austin, TX, USA) was used to analyze amplifier signals. Combined, this system enabled feedback positional control of the nanoelectrode through micro-manipulation, piezoelectric stage positioning, ion conductance monitoring, and data acquisition.

Probe Development

The probe was prepared from fire-polished, thin-wall borosilicate glass capillaries (O.D. 1.0 mm, I.D. 0.78 mm, Sutter instrument, Novato, CA, USA) with an internal electrode filament (Fig. 1 middle). The capillary was pulled with a PUL-1 micropipette puller (World Precision Instruments, Florida, USA) so that the pipette had a shank as short as possible in order for it to resist deflection during nano-manipulation, while maintaining a small tip size (Fig. 1 middle). Finite element analysis of tip deformation showed that the lateral spring constant was about 100 nN/nm (data not shown). Taper length was found to correlate inversely with probe diameter, meaning the longer the taper length, the smaller the probe diameter (data not shown). The probes were fabricated such that tip inner radii were approximately 250 nm for a "small" (Fig. 1 middle), 500 nm for a "medium", and 1 μm for a "large" sized probe, as verified by electron microscopy. The electrode resistance was < 50 MΩ.

Probe Set-up

In order to minimize interference with the optical light path of the microscope, the capillary was bent by approximately 45° using the heated filament of the PUL-1 puller thereby decreasing obstruction of phase contrast microscopy. The tip was filled by capillary action along the inner filament of the glass pipette.

The back of the probe was first immersed into CO_2-independent media and allowed to passively back fill for approximately 1 min. The remaining tapered region was back filled using a 34 gauge MicroFil (World precision instruments, Inc. Sarasota, FL, USA). Two electrode holders were tested, the QSW-A10P (Warner Instruments, Hamden, CT, USA) which uses a Ag wire, and the KCl bridge electrode holder (model ALA PPH-KCL-BNC, ALA Scientific Instruments, Inc., Westbury, NY, USA).[54] The latter was used for the functionalized probe experiments as it had a more stable DC current (less drift) and less noise (data not shown).

Fibronectin Functionalization of the Nanoelectrode

Fibronectin (FN) was diluted with DPBS under sterile conditions to concentrations of 0, 0.01, 0.05, 0.1, and 0.5 mg/ml. All functionalization steps, including incubation, were carried out inside a cell culture hood under sterile conditions. Borosilicate glass nanoelectrode probes were cleaned in H_2O/EtOH 80% (v/v) solution and rinsed twice in autoclaved ddH_2O. The tips were filled with CO_2-independent media, and micropipettes were placed in holders. Tips were then submerged in FN solution and the setup was then placed inside a 37 °C incubator for 4 h. When necessary, visualization of the functionalized nanoelectrode was achieved by fluorescently labeling FN using the AlexaFluor 568 Protein Labeling Kit (Molecular Probes A10238) (Fig. 1 middle).

In order to find the optimal concentration for binding of the nanoelectrode probe, probes functionalized using FN concentrations of 0, 0.01, 0.05, 0.1, or 0.5 mg/ml were brought to the cell, allowed to bind, and the ion current was monitored during the retraction phase, (t_3 in Fig. 1, bottom). Specifically, the probe was halted when the initial current dropped by 2% (e.g., from 2.02 to 1.98 nA) while a 1 mV V_m was applied. This % current drop ensured cell contact was made with minimal indentation and falls between the < 2% drop in current used in non-contact mode SICM and the drop of 20% used in patch clamp indentation experiments. After contact, binding was assessed by measuring the current during retraction of the probe after 10 min of reaction time.

Cell Culture and Transfections

All *in vitro* experiments were performed on bovine aortic endothelial cells (BAECs) (VEC technologies, Rensselaer, NY). BAECs were sub-cultured between passages 3–10 in T-25 flasks with MCDB-131 complete medium (VEC technologies, Rensselaer, NY) while maintained at 37 °C in a gas mixture of 95% air and

5% CO_2 with 90% humidity. The cells were then seeded onto chambered coverglasses and placed in the incubator for 2 h, after which new MCDB-131 media was added. BAECs were incubated overnight. Cellular transfection of red fluorescent protein (RFP)-talin fusion sequences were performed the day before imaging using BacMam technology (Invitrogen) at a ratio of approximately 10 particles of BacMam per cell.

Assessing Probe-Induced Focal Adhesion Assembly

In order to measure the time course of molecular-scale activation in newly formed focal adhesions, the FN-functionalized probe was allowed to come into contact with BAECs transfected with RFP-talin. Probes were positioned over the cell to be contacted, the cell was raised to meet the tip of the probe using the piezoelectric stage, while monitoring the current between the tip and the cell as the approach phase (t_1) progressed (Fig. 1, bottom). After contact, as recognized by the electronic signature of the approach phase, the reaction phase (t_2) began and the FN-functionalized tip was allowed to bind to the cell for intervals of 0, 1, 5, 10, and 15 min. The third phase was retraction (t_3), where the cell was moved away from the probe using the piezoelectric stage, while monitoring the current between the probe and the cell. To assess talin accumulation, time-lapsed confocal images of RFP fluorescence were collected during the adhesion phase.

Data Analysis and Statistics

Images were processed using ImageJ software. Average pixel values in regions of interest of time-lapse images remote from the probe contact point were determined in order to characterize degradation of RFP fluorescence due to photobleaching. These average values were added back to values of RFP fluorescence evaluated at the probe site. The resulting values were then normalized to initial intensity and then plotted with respect to time. Where indicated, compiled data is represented as mean ± standard deviation. Statistical significance was evaluated using a Student's t-test at the $p < 0.05$ level.

RESULTS

Defining Probe-Cell Contact

A 2% decrease (e.g., 0.04 nA) from the initial current (e.g., 2.02 nA) was used to define the timing of probe-cell contact. This 2% decrease was 4 times greater than the system noise, calculated at 0.01 nA (RMS). For an approach phase slope of 0.25 nA/μm,
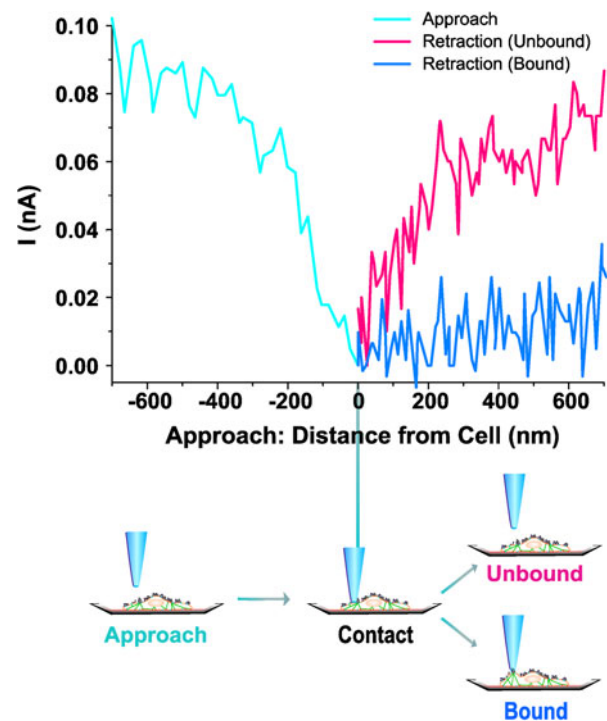

FIGURE 2. **Approach of probe to the cell. This figure depicts the changes in current accompanying the last few nanometers of approach and retraction. During the approach phase, the piezoelectric stage moved the cell towards the probe and the current of the nanoelectrode was continuously monitored. The current displayed a marked decrease once the probe was near the cell surface, and achieved probe-cell contact as defined by a 2% total percentage drop from the initial current value. During the retraction phase, the piezo-electric stage moved the cell away from the probe and the current increased when the probe was retracted from the cell surface. For a cell that was bound to the probe, current did not increase during retraction.**

the uncertainty in position of contact was approximately 40 nm (RMS/slope). The decrease in current began when the probe was within 500 nm of cell surface (Fig. 2). Once contact was achieved, the position of the probe and the cell was maintained. In control experiments using a non-functionalized electrode, retraction of the probe resulted in an increase in current that mirrored the decrease of current during the approach phase (Fig. 2), whereas current was maintained after retraction of functionalized probes. These results demonstrate that current transients were good indicators of adhesion.

Nascent Focal Adhesion Formation

The FN-functionalized nanoelectrode probe was allowed to come into contact with the cell using the electronic signature shown in Fig. 2. After probe-cell contact, the reaction phase took place, allowing for the induction of a nascent focal adhesion at the site of
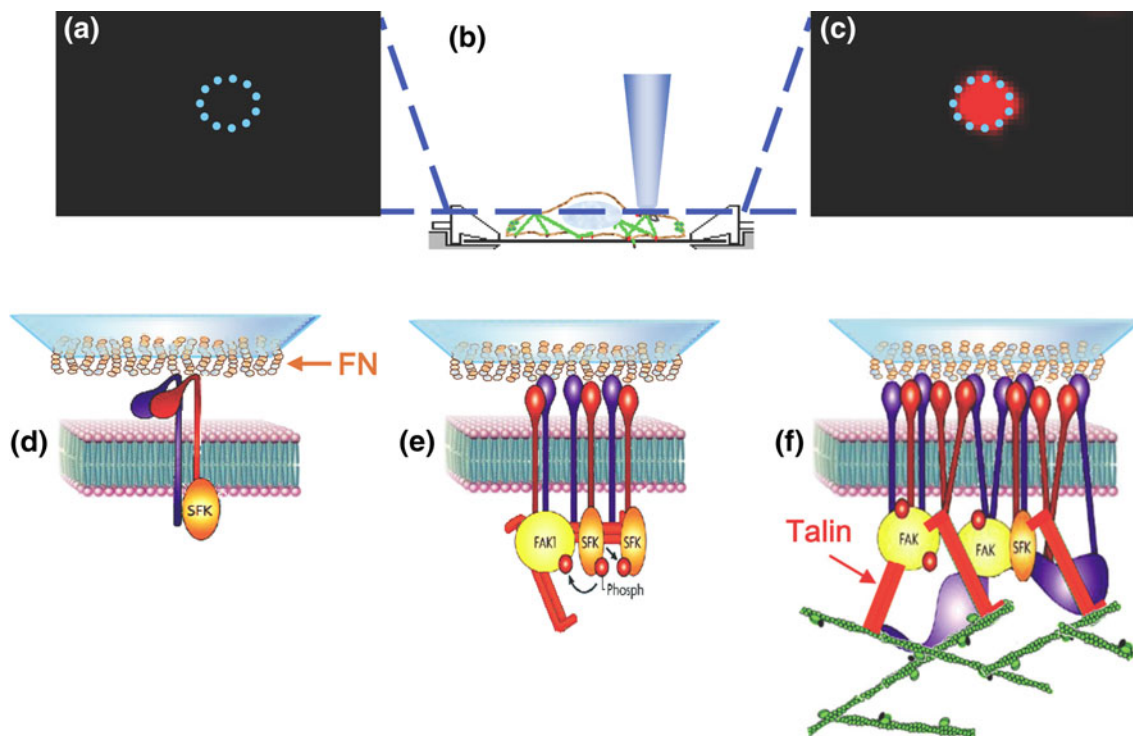
FIGURE 3. Induction of focal adhesions upon probe contact: Confocal images at the apical surface verify nascent focal adhesion formation (a and c). At the time the probe made contact with the cell ($t = 0$) (a) no RFP-talin was present on the apical surface of the cell at the probe-cell contact site (circle). After a reaction phase of $t = 15$ min (b) during which the fibronectin-functionalized probe remained in contact with the cell, presence of an induced apical nascent focal adhesion was observed *via* accumulation of RFP-talin at the site of probe cell contact (c, circle). This induction likely followed outside-in signaling *via* integrins induced by the fibronectin functionalized probe (d, e, f). (SFK-Src Family Kinase, FAK-Focal Adhesion Kinase).

probe-cell contact. The time of contact was defined as $t = 0$. Initially, there was no evidence of a focal adhesion at the probe tip (Fig. 3a). However, over a total reaction time of 15 min, the time lapsed images (Fig. 3c) of red fluorescence indicated the accumulation of talin resulting from the formation of a nascent focal adhesion at the site of probe-cell contact. Accumulation of talin is a marker for activated integrins, which bind to FN during focal adhesion formation (illustrated in Figs. 3d–3f). Thus, in addition to the electronic signature during approach, talin accumulation provides unambiguous verification of probe-cell contact and binding.

Remote Remodeling of Focal Adhesions

Upon contact, the time-lapsed images of RFP-talin revealed not only the induction of an apical focal adhesion at the probe site (circle) as seen in Fig. 3c and in Fig. 4 ($t = 80$ s), but also the remote remodeling of basal focal adhesion sites. A z-stack of confocal images was used to distinguish between apical vs. basal focal adhesion sites. Selected time points allowed for the concurrent visualization of initial focal adhesion sites pseudo-colored in blue at time $t = 0$ s (contact time),

and real-time location of focal adhesion sites pseudo-colored in red during the reaction time of 15 min. The overlay of initial locations (blue) and subsequent locations (red) can be seen in each of the panels of Fig. 4. By $t = 20$ s remodeling of basal focal adhesion sites was evident. Partial overlap is denoted by the purple region at $t = 20$ s and $t = 40$ s. At $t = 60$ s complete translocation of basal focal adhesion sites occurred, as all sites had new locations. Notably, at time $= 80$ s, RFP-talin accumulation at the probe tip was observed, suggesting that a nascent apical focal adhesion was forming at the site of probe-cell contact (circle). At subsequent time points ($t = 3$ min to $t = 15$ min) continued remodeling of remote basal focal adhesion sites occurred in response to probe-cell contact and binding. Non-contacted control cells did not exhibit appreciable basal remodeling over the 15 min observation time (data not shown).

Kinetics of Talin Accumulation

Using an image frame rate of 2 s^{-1}, the kinetics of RFP-talin accumulation was assayed during the first 90 s of formation of the nascent focal adhesion. Average fluorescence intensity was measured for each time
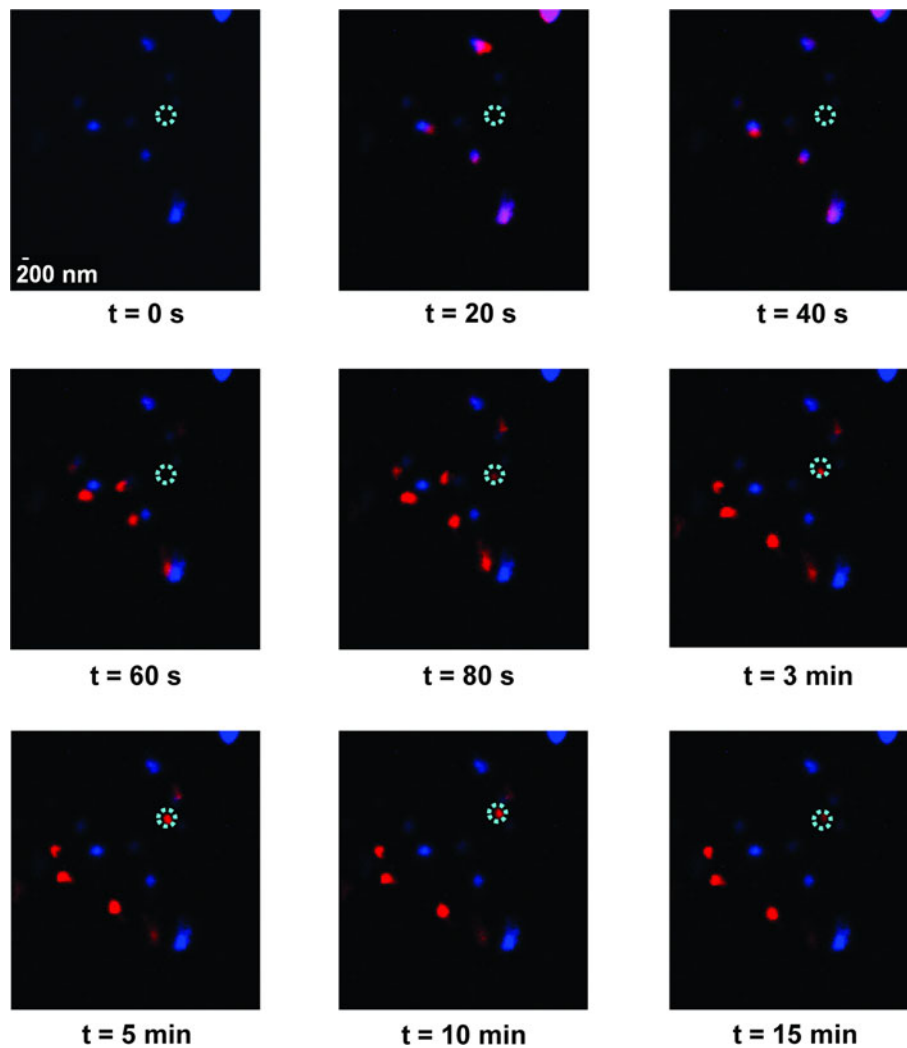
FIGURE 4. Real-time response of basal focal adhesions to apical probe-cell contact during reaction phase. Selected time-lapse images of RFP-talin display concurrent initial location of focal adhesion sites (pseudo-colored in blue at $t = 0$ or contact time) overlaid with real time location of sites (pseudo-colored in red). At time = 0 s, no accumulation of RFP-talin at the probe site (circle) was evident. Remodeling of remote basal focal adhesion sites was observed in response to contact as early as the first time point of 20 s and throughout the reaction time of 15 min. At time = 80 s a nascent apical focal adhesion site was observed at the site of probe-cell contact. Subsequent time points ($t = 3$ min to $t = 15$ min) displayed continued remodeling and translocation of remote basal focal adhesion sites.
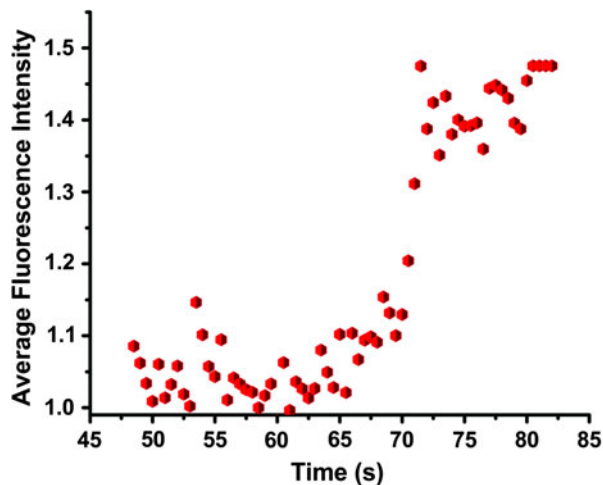
point, corrected for photobleaching and normalized to initial values. The accumulation profile for talin as seen in Fig. 5 displays delayed accumulation followed by a rapid increase starting at 65 s and reaching a plateau at 82 s. The average fluorescent intensity increased by approximately 50% from its initial value. These results demonstrate that the ability to monitor the kinetics of formation of the nascent focal adhesion site subsequent to a precisely defined initial contact time point.

Further Verification of Probe-Cell Binding

The slope of the retraction electronic signature, images from phase microscopy, and confocal

fluorescence verified that current failed to increase upon retraction of a bound probe whereas current increased upon retraction when the probe was not bound (Fig. 6a). Even at a distance of 5 μm from the initial point of contact, the electronic signature was able to distinguish between a bound and an unbound cell. Concurrently, brightfield images were able to show that if the probe was displaced further, the cell remained bound to the probe (Figs. 6b–6c). Fluorescence images of RFP-talin showed that when the probe was moved laterally, the focal adhesion moved with it (Figs. 6d–6e). These results suggest that electrode current can be used to monitor the extend of binding even during deformation of the cell by the probe.

FIGURE 5. Time course of talin accumulation at probe site. Time course of transfected RFP-talin was measured using average fluorescence intensity at the probe site. Following probe contact with the cell, there was little to no accumulation for about 65 s. Subsequently, talin accumulated rapidly reaching a 50% increase which plateaued at 82 s.

Optimization of Probe-Cell Binding

Lastly, a few key parameters were optimized. For SICM imaging and probe positioning, the scanning image resolution and sensitivity depends on the tip diameter and shape. Since the potential to bind to the cell also depends on the probe size, we determined the effect of the probe tip size on the ion current pattern of phase t_3. We categorized the probe tip sizes as "small," corresponding to a tip radius <250 nm and probe electrical resistance >20 MΩ, and "medium," corresponding to tip radii between 250 and 500 nm with a probe electrical resistance of 10–20 MΩ. Experiments were conducted with different reaction times (1, 5, and 10 min) and with different FN concentrations (0.01, 0.05, and 0.1 mg/ml). First, increasing FN concentration decreased the slope of the current vs. retraction distance curve (Fig. 7a). Thus the slope can be used to assess degree of adhesion. Second, as shown in Fig. 7b, the success rate increased as the FN concentration increased. With a 10 min reaction phase, a medium
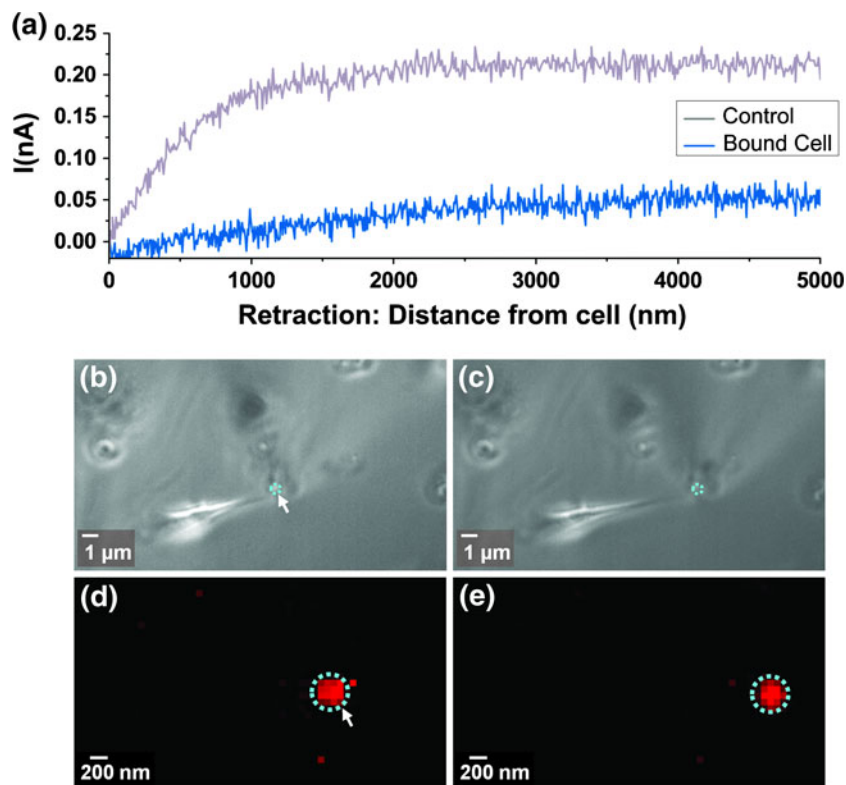
FIGURE 6. Verification of probe-cell binding at nascent focal adhesion: Three simultaneous metrics were used to verify that the probe remained bound to the cell through the induced nascent focal adhesion. (a) Current increases upon probe retraction from cells were substantially smaller for a bound cell (bottom curve) vs. an unbound cell (top curve). Final current value was subtracted from raw current values so that each curve would start at 0 nA. (b, c) Phase contrast images demonstrate that the cell remained bound to the probe. (d, e) Fluorescence microscopy images reveal that the focal adhesion remained bound to the probe as the probe was moved during lateral displacement.
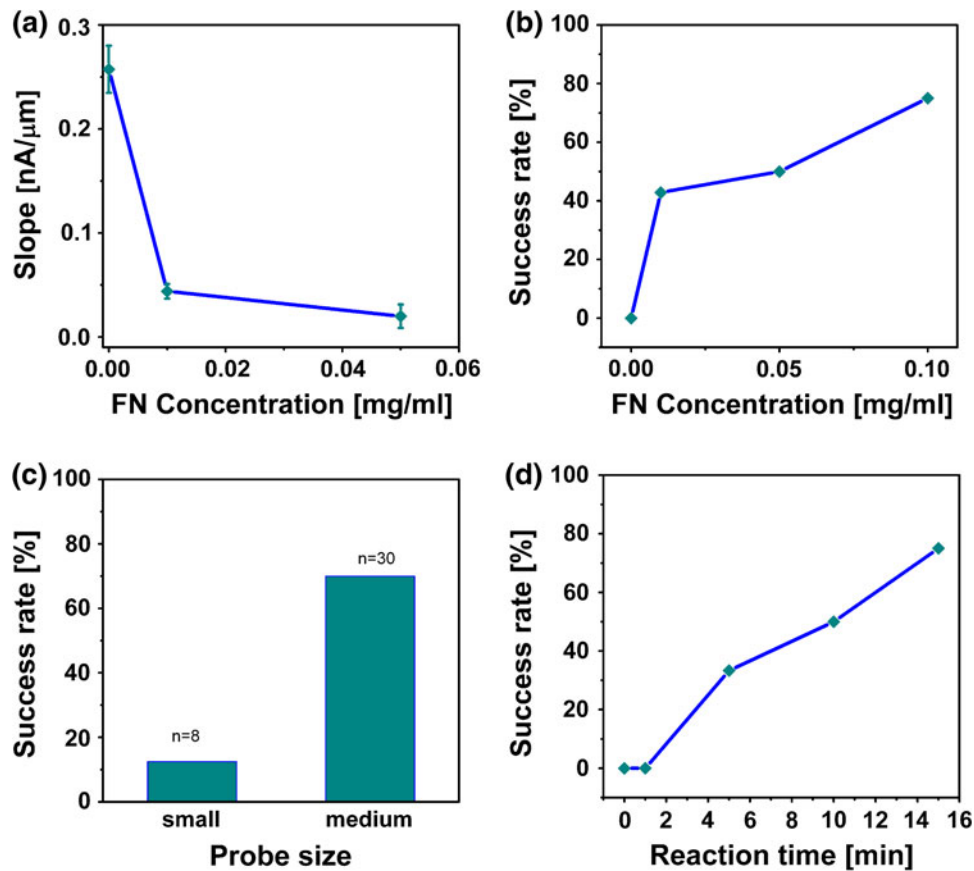
FIGURE 7. Parameters affecting probe-cell binding: (a) Slope of current vs. retraction distance after binding as a function of fibronectin concentration. Small slope indicates tighter binding between pipette and cell surface. (b) Success rate of binding increases as a function of fibronectin concentration (c) Binding success rate increases as probe size increases, (d) Increased reaction time increases success rate of binding.

probe size, and 1 mV V_m, the success rates were 42.8, 50, and 75% at FN concentrations of 0.01, 0.05, and 0.1 mg/ml, respectively. Third, successful probe-cell binding was observed to be dependent on probe size (Fig. 7c). With 0.01 mg/ml of FN, 10 min of reaction time, and 1 mV V_m, the success rates for binding were 12.5% and 70% for using small and medium sized probes, respectively. Finally, we determined the effect of reaction time on the success rate of binding. As shown in Fig. 7d, the success rate increased as the FN reaction time increased. With 0.05 mg/ml FN concentration, medium probe size, and 1 mV V_m, the success rates were 0, 33.3, and 50% for reaction times of 0, 5, and 10 min, respectively.

DISCUSSION

The main findings of this study are that ion conductance through a nanoelectrode can be used to prescribe the time and location of induction of a focal adhesion, induced focal adhesions can be mechanically manipulated, and current transients through the electrode provide a readout of the degree and integrity of adhesion. These findings were supported by assays for focal adhesion formation and remodeling indicated by fluorescently labeled talin, which accumulates at focal adhesion sites subsequent to activation and dimerization of integrins.[1,3,7,9,10] This technique was designed to enable detailed delineation of the identity and kinetics of the numerous proteins that participate in focal adhesion formation and reinforcement upon mechanical manipulation.

Focal contacts undergo a series of remodeling steps during the process of maturing into focal adhesions.[8] Once matured, structural proteins are recruited including integrins, extracellular matrix proteins such as fibronectin, vitronectin, laminin, and intracellular proteins such as talin and vinculin. Integrin activation is essential for the initiation of focal adhesions in that conformational reorganization of the integrin dimer increases its affinity to the matrix ligand.[55] This activation is associated with integrin recognition by talin[17,23] and results in binding of talin to the cytoplasmic

domains of integrins and connection with the actin cytoskeleton.[20,24,55] Focal adhesions can be induced by outside-in signaling, they function as both adhesion and signal transduction organelles, and they serve to inform the cell about the chemical makeup and mechanics of its surroundings.

Focal adhesions form due to accumulation of focal adhesion proteins and it is believed that focal adhesion proteins, themselves, are sensitive to applied forces. For example, Bell,[5] proposed that the rate constant governing receptor-ligand binding was dependent on mechanical force. Numerous other studies have elucidated tethering bond kinetics, slip bonds, catch bonds, and unbinding kinetics[13,33,36,37] of focal adhesion proteins.[4,36,52] Less well understood is the dependence on force of the kinetics of accumulation of focal adhesion proteins, especially during the initial stages of focal adhesion formation. Although previous studies have provided insight into the development of focal adhesions from nascent focal contacts,[4,36,52] there are no published reports of the kinetics of focal contact formation in response to adhesion, likely due to the difficulty in defining the initial contact time. In this study we introduce a technique in which induction of focal contact formation is precisely timed and provide preliminary data on the real-time kinetics of talin accumulation in response to initial probe cell contact, in a spatially localized manner. We also show that the same electrode can be used to apply a prescribed deformation to the newly formed focal adhesion.

This study is based on SICM and provides a means for outside-in induction of a single nascent apical focal adhesion in a single bovine aortic endothelial cell using nanoelectrode probe-cell contact. SICM was invented by Hansma *et al.*,[28] and has been further developed to image and analyze surface topography of live cells. SICM is a non-optical imaging method that uses an electrolyte-filled nanopipette as a scanning probe to image cell surface structures with resolution at the nanometer level. SICM records the ionic current through the probe as the probe is scanned over the surface of a sample immersed in an electrolyte solution. The current drop used in SICM to define probe cell contact is typically 2% or less of the initial current. SICM employs a feedback loop to maintain a constant distance between the pipette and the surface, so that the displacement of the scanning pipette normal to the sample during a scan represents the topography of the surface.

While SICM emphasizes the non-contact nature of probe positioning, we have functionalized our nanopipette and used the positioning sensitivity (on the order of 40 nm) to minimally contact the cell surface with molecular specificity. In addition, by using the electronic signature of the nanopipette electrode, we can assess the integrity of the attachment of the cell surface

with the pipette, in real time, and monitor detachment. A previous study by Riveline *et al.*[49] also used nanopipettes functionalized with fibronectin for cell manipulation. In that study, remote focal adhesions moved toward the pipette in response to large mechanical perturbation of the cell surface. This observation is in contrast with focal adhesion movement away from the probe observed in our experiments. It is possible that the large deformations used in the Riveline caused focal adhesion translocation in the direction of the force, which in the large deformation case, is toward the pipette. In the current study, focal adhesions translocated without applied force. Therefore, it is possible that the new adhesion point induced by the pipette led to cytoskeletal remodeling and subsequent changes in force distribution in the cell. Although it would be difficult to predict the directions of forces in this instance, these changes in force distribution could have led to basal focal adhesion remodeling. Consistent with this interpretation, in related studies by Mathur *et al.*,[38,39] remote sensing of basal focal adhesions in response to small forces applied by AFM showed that that the cell responds globally to the localized applied force. Our results, therefore, are consistent with other's observations[15,40,57] that focal adhesions respond to applied external force. However, our method explores the additional phenomenon of the response of the cell to minimal force application. It uses SICM technology to provide a new tool for timed induction of focal adhesions with nm-scale deformation ranging from near zero nm to micron scale. Such studies will be useful in elucidating the early events of focal adhesion formation and reinforcement in response to force.

SICM is a technique complementary to AFM for assessing topography of cells, and to optical and magnetic tweezers for force application. For example, the AFM, a member of the scanning probe family of microscopes, manipulates a cantilevered probe (tip radius ranging from a few nanometers to a few micrometers) for tension or compression loading.[29,47,51] A slightly larger version of the AFM technique facilitates microscale indentation of an entire cell.[32,35] Conventional AFM can detect forces in the range of 10–100 pN and has a displacement range of 0.5–100 nm. One disadvantage of AFM is that it is difficult to study biological processes and structures non-intrusively since by definition the cantilever must be deflected in order to define contact.[42] In our implementation of SICM, current through the electrode provides the distance measurement and contact is initiated only at prescribed times and locations.

Optical tweezers, can measure forces on a μm scale bead of up to 100 pN[41,48] with sub-millisecond temporal resolution. When the laser beam is focused on a dielectric particle, the particle experiences a

three-dimensional restoring force directed toward the center of the focused beam.[2,48] Even though optical tweezers have high versatility and precision, focused laser light can induce cell damage caused by local heating.[42,46,53] More importantly, trap stiffness depends on the gradient of the optical field, which can be refracted by contaminating substances and adherent cells. Magnetic tweezers, on the other hand, use a magnetic field gradient to exert and measure pico- to nanonewton forces on magnetic particles.[26,42] The core advantage of magnetic tweezers is that it permits parallel single-bead measurement because a magnetic field can exert force everywhere, which would be difficult to achieve with other force spectroscopy techniques.[18] Some limitations are that the bandwidth and sensitivity are limited by video-based detection and high-current electromagnets can generate undesirable Joule heating.[14,42] Studies such as optical and magnetic tweezers which use particles as probes[30] must also contend with internalization of particles due to phagocytosis, the relatively non-uniform distribution of beads, and large (3–6 μm^2) and ambiguous contact area between the bead and cell membrane.[43] In contrast, the nanoelectrode probe used in this study cannot be phagocytosed or pulled due to its shape and stiffness.

SUMMARY

In summary, we introduce a new method for induction and manipulation of a focal adhesion on a single endothelial cell using a functionalized nanoelectrode probe. We observed that binding of the probe onto the cell surface was dependent on the nanoelectrode size, fibronectin concentration, and binding reaction time between probe and cell, which was accomplished through integrin-fibronectin linkages. Furthermore, by coupling the technique with high speed confocal microscopy, we show that it is possible to assess the dynamics of assembly of the individual constituents of focal adhesions from the moment of probe contact onward. This new capability should allow for the development of new kinetic models of focal adhesion assembly in the presence and absence of force, thus opening up new areas of research in the integration of engineering principles of molecular transport and biological sensing of the cellular microenvironment.

REFERENCES

[1]Anthis, N. J., K. L. Wegener, F. Ye, C. Kim, B. T. Goult, E. D. Lowe, I. Vakonakis, N. Bate, D. R. Critchley, M. H. Ginsberg, and I. D. Campbell. The structure of an integrin/ talin complex reveals the basis of inside-out signal transduction. *EMBO J.* 28:3623–3632, 2009.

[2]Ashkin, A., J. M. Dziedzic, and T. Yamane. Optical trapping and manipulation of single cells using infrared laser beams. *Nature* 330:769–771, 1987.

[3]Askari, J. A., P. A. Buckley, A. P. Mould, and M. J. Humphries. Linking integrin conformation to function. *J. Cell Sci.* 122:165–170, 2009.

[4]Baneyx, G., L. Baugh, and V. Vogel. Fibronectin extension and unfolding within cell matrix fibrils controlled by cytoskeletal tension. *Proc. Natl Acad. Sci.* 99:5139–5143, 2002.

[5]Bell, G. I. Models for the specific adhesion of cells to cells. *Science* 200:618–627, 1978.

[6]Binnig, G., C. F. Quate, and C. Gerber. Atomic force microscope. *Phys. Rev. Lett.* 56:930–933, 1986.

[7]Bouaouina, M., Y. Lad, and D. A. Calderwood. The N-terminal domains of talin cooperate with the phosphotyrosine binding-like domain to activate beta1 and beta3 integrins. *J. Biol. Chem.* 283:6118–6125, 2008.

[8]Butcher, D. T., T. Alliston, and V. M. Weaver. A tense situation: forcing tumour progression. *Nat. Rev. Cancer* 9:108–122, 2009.

[9]Calderwood, D. A. Integrin activation. *J. Cell Sci.* 117: 657–666, 2004.

[10]Campbell, I. D., and M. H. Ginsberg. The talin-tail interaction places integrin activation on FERM ground. *Trends Biochem. Sci.* 29:429–435, 2004.

[11]Castelain, M., F. Pignon, J. M. Piau, A. Magnin, M. Mercier-Bonin, and P. Schmitz. Removal forces and adhesion properties of Saccharomyces cerevisiae on glass substrates probed by optical tweezer. *J. Chem. Phys.* 127: 135104, 2007.

[12]Celedon, A., I. M. Nodelman, B. Wildt, R. Dewan, P. Searson, D. Wirtz, G. D. Bowman, and S. X. Sun. Magnetic tweezers measurement of single molecule torque. *Nano. Lett.* 9:1720–1725, 2009.

[13]Chen, S., and T. A. Springer. Selectin receptor ligand bonds: formation limited by shear rate and dissociation governed by the Bell model. *Proc. Natl Acad. Sci.* 98:950–955, 2001.

[14]Chiou, C. H. A micromachined DNA manipulation platform for the stretching and rotation of a single DNA molecule. *J. Micromech. Microeng.* 15:109, 2005.

[15]Choquet, D., D. P. Felsenfeld, and M. P. Sheetz. Extracellular matrix rigidity causes strengthening of integrin-cytoskeleton linkages. *Cell* 88:39–48, 1997.

[16]Cluzel, P., A. Lebrun, C. Heller, R. Lavery, J. L. Viovy, D. Chatenay, and F. Caron. DNA: an extensible molecule. *Science* 271:792–794, 1996.

[17]Critchley, D. R., and A. R. Gingras. Talin at a glance. *J. Cell Sci.* 121:1345–1347, 2008.

[18]Danilowicz, C., D. Greenfield, and M. Prentiss. Dissociation of ligand-receptor complexes using magnetic tweezers. *Anal. Chem.* 77:3023–3028, 2005.

[19]Davies, P. F., J. Zilberberg, and B. P. Helmke. Spatial microstimuli in endothelial mechanosignaling. *Circ. Res.* 92:359–370, 2003.

[20]de Pereda, J. M., K. L. Wegener, E. Santelli, N. Bate, M. H. Ginsberg, D. R. Critchley, I. D. Campbell, and R. C. Liddington. Structural basis for phosphatidylinositol phosphate kinase type Igamma binding to talin at focal adhesions. *J. Biol. Chem.* 280:8381–8386, 2005.

[21]Eibl, R. H., and V. T. Moy. Atomic force microscopy measurements of protein-ligand interactions on living cells. *Methods Mol. Biol.* 305:439–449, 2005.

[22]Evans, E., K. Ritchie, and R. Merkel. Sensitive force technique to probe molecular adhesion and structural linkages at biological interfaces. *Biophys. J.* 68:2580–2587, 1995.

[23]Garcia-Alvarez, B., J. M. de Pereda, D. A. Calderwood, T. S. Ulmer, D. Critchley, I. D. Campbell, M. H. Ginsberg, and R. C. Liddington. Structural determinants of integrin recognition by talin. *Mol. Cell.* 11:49–58, 2003.

[24]Geiger, B., J. P. Spatz, and A. D. Bershadsky. Environmental sensing through focal adhesions. *Nat. Rev. Mol. Cell Biol.* 10:21–33, 2009.

[25]Gorelik, J., Y. Zhang, A. I. Shevchuk, G. I. Frolenkov, D. Sanchez, M. J. Lab, I. Vodyanoy, C. R. W. Edwards, D. Klenerman, and Y. E. Korchev. The use of scanning ion conductance microscopy to image A6 cells. *Mol. Cell. Endocrinol.* 217:101–108, 2004.

[26]Gosse, C., and V. Croquette. Magnetic tweezers: micromanipulation and force measurement at the molecular level. *Biophys. J.* 82:3314–3329, 2002.

[27]Gosse, C., and V. Croquette. Magnetic tweezers: micromanipulation and force measurement at the molecular level. *Biophys. J.* 82:3314–3329, 2002.

[28]Hansma, P., B. Drake, O. Marti, S. Gould, and C. Prater. The scanning ion-conductance microscope. *Science* 243:641–643, 1989.

[29]Hassan, E., W. F. Heinz, M. D. Antonik, N. P. D'Costa, S. Nageswaran, C. A. Schoenenberger, and J. H. Hoh. Relative microelastic mapping of living cells by atomic force microscopy. *Biophys. J.* 74:1564–1578, 1998.

[30]Huang, H., R. D. Kamm, and R. T. Lee. Cell mechanics and mechanotransduction: pathways, probes, and physiology. *Am. J. Physiol. Cell Physiol.* 287:C1–C11, 2004.

[31]Kegler, K., M. Salomo, and F. Kremer. Forces of interaction between DNA-grafted colloids: an optical tweezer measurement. *Phys. Rev. Lett.* 98:058304, 2007.

[32]Koay, E. J., A. C. Shieh, and K. A. Athanasiou. Creep indentation of single cells. *J. Biomech. Eng.* 125:334–341, 2003.

[33]Konstantopoulos, K., W. D. Hanley, and D. Wirtz. Receptor-ligand binding: [']catch' bonds finally caught. *Curr. Biol.* 13:R611–R613, 2003.

[34]Korchev, Y., C. Bashford, M. Milovanovic, I. Vodyanoy, and M. Lab. Scanning ion conductance microscopy of living cells. *Biophys. J.* 73:653–658, 1997.

[35]Leipzig, N. D., and K. A. Athanasiou. Unconfined creep compression of chondrocytes. *J. Biomech.* 38:77–85, 2005.

[36]Lele, T. P., C. K. Thodeti, and D. E. Ingber. Force meets chemistry: Analysis of mechanochemical conversion in focal adhesions using fluorescence recovery after photobleaching. *J. Cell. Biochem.* 97:1175–1183, 2006.

[37]Marshall, B. T., M. Long, J. W. Piper, T. Yago, R. P. McEver, and C. Zhu. Direct observation of catch bonds involving cell-adhesion molecules. *Nature* 423:190–193, 2003.

[38]Mathur, A. B., G. A. Truskey, and W. Monty Reichert. Total internal reflection microscopy and atomic force microscopy (TIRFM-AFM) to study stress transduction mechanisms in endothelial cells. *Crit. Rev. Biomed. Eng.* 28:197–202, 2000.

[39]Mathur, A. B., G. A. Truskey, and W. Monty Reichert. Atomic force and total internal reflection fluorescence microscopy for the study of force transmission in endothelial cells. *Biophys. J.* 78:1725–1735, 2000.

[40]Matthews, B. D., D. R. Overby, F. J. Alenghat, J. Karavitis, Y. Numaguchi, P. G. Allen, and D. E. Ingber. Mechanical properties of individual focal adhesions probed with a magnetic microneedle. *Biochem. Biophys. Res. Commun.* 313:758–764, 2004.

[41]Moffitt, J. R., Y. R. Chemla, D. Izhaky, and C. Bustamante. Differential detection of dual traps improves the spatial resolution of optical tweezers. *Proc. Natl Acad. Sci. USA.* 103:9006–9011, 2006.

[42]Neuman, K. C., and A. Nagy. Single-molecule force spectroscopy: optical tweezers, magnetic tweezers and atomic force microscopy. *Nat. Methods* 5:491–505, 2008.

[43]Ohayon, J., P. Tracqui, R. Fodil, S. Fereol, V. M. Laurent, E. Planus, and D. Isabey. Analysis of nonlinear responses of adherent epithelial cells probed by magnetic bead twisting: a finite element model based on a homogenization approach. *J. Biomech. Eng.* 126:685–698, 2004.

[44]Orr, A. W., B. P. Helmke, B. R. Blackman, and M. A. Schwartz. Mechanisms of mechanotransduction. *Dev. Cell* 10:11–20, 2006.

[45]Panhorst, M., P. B. Kamp, G. Reiss, and H. Bruckl. Sensitive bondforce measurements of ligand-receptor pairs with magnetic beads. *Biosens. Bioelectron.* 20:1685–1689, 2005.

[46]Peterman, E. J. G., F. Gittes, and C. F. Schmidt. Laser-induced heating in optical traps. *Biophys. J.* 84:1308–1316, 2003.

[47]Radmacher, M. Measuring the elastic properties of biological samples with the AFM. *IEEE Eng. Med. Biol. Mag.* 16:47–57, 1997.

[48]Rief, M., F. Oesterhelt, B. Heymann, and H. E. Gaub. Single molecule force spectroscopy on polysaccharides by atomic force microscopy. *Science* 275:1295–1297, 1997.

[49]Riveline, D., E. Zamir, N. Q. Balaban, U. S. Schwarz, T. Ishizaki, S. Narumiya, Z. Kam, B. Geiger, and A. D. Bershadsky. Focal contacts as mechanosensors: externally applied local mechanical force induces growth of focal contacts by an mDia1-dependent and ROCK-independent mechanism. *J. Cell Biol.* 153:1175–1186, 2001.

[50]Roichman, Y., V. Wong, and D. G. Grier. Colloidal transport through optical tweezer arrays. *Phys. Rev. E. Stat. Nonlin. Soft. Matter Phys.* 75:011407, 2007.

[51]Rotsch, C., and M. Radmacher. Drug-Induced changes of cytoskeletal structure and mechanics in fibroblasts: an atomic force microscopy study. *Biophys. J.* 78:520–535, 2000.

[52]Sawada, Y., and M. P. Sheetz. Force transduction by Triton cytoskeletons. *J. Cell Biol.* 156:609–615, 2002.

[53]Seol, Y., A. E. Carpenter, and T. T. Perkins. Gold nanoparticles: enhanced optical trapping and sensitivity coupled with significant heating. *Opt. Lett.* 31:2429–2431, 2006.

[54]Snyder, K. V., A. M. Kriegstein, and F. Sachs. A convenient electrode holder for glass pipettes to stabilize electrode potentials. *Pflugers Arch.* 438:405–411, 1999.

[55]Tadokoro, S., S. J. Shattil, K. Eto, V. Tai, R. C. Liddington, J. M. de Pereda, M. H. Ginsberg, and D. A. Calderwood. Talin binding to integrin beta tails: a final common step in integrin activation. *Science* 302:103–106, 2003.

[56]Tanase, M., N. Biais, and M. Sheetz. Magnetic tweezers in cell biology. *Methods Cell Biol.* 83:473–493, 2007.

[57]Wang, Y., E. L. Botvinick, Y. Zhao, M. W. Berns, S. Usami, R. Y. Tsien, and S. Chien. Visualizing the mechanical activation of Src. *Nature* 434:1040–1045, 2005.

[58]Wolenski, J. S., R. E. Cheney, M. S. Mooseker, and P. Forscher. In vitro motility of immunoadsorbed brain myosin-V using a Limulus acrosomal process and optical tweezer-based assay. *J. Cell Sci.* 108(Pt 4):1489–1496, 1995.